THE ASTROPHYSICAL JOURNAL, 468:79–85, 1996 September 1

TEMPERATURE AND METALLICITY OF A MASSIVE X-RAY CLUSTER AT REDSHIFT 0.5

MEGAN DONAHUE
Space Telescope Science Institute, 3700 San Martin Drive, Baltimore, MD 21218; donahue@stsci.edu
Received 1995 July 26; accepted 1996 March 19

ABSTRACT

We present spectroscopic X-ray observations, obtained with the *Advanced Satellite for Cosmology and Astrophysics (ASCA)*, of MS 0451.6−0305, the most luminous cluster of galaxies and one of the most distant ($z = 0.54$) in the Extended Medium-Sensitivity Survey (EMSS). We find that the hot gas in this cluster has a temperature of 10.4 ± 1.2 keV, which is very hot but commensurate with its X-ray luminosity (2–10 keV rest frame) of $2.2 \times 10^{45}\ h_{50}^{-2}$ ergs s^{-1}, if the relationship between L_x and T_x is the same at redshift 0.5 as nearby. The iron abundance of this gas is $0.15^{+0.11}_{-0.12}$ solar, somewhat lower than, but consistent with, the iron abundance of hot gas in nearby clusters. The temperature of this gas, when combined with the image parameters of the *ROSAT* Position Sensitive Proportional Counter (PSPC) X-ray map and with the assumption that the gas is isothermal and in nearly hydrostatic equilibrium with the cluster gravitational potential, implies a hot gas mass of $4.1 \times 10^{13}\ h_{50}^{-5/2}\ M_\odot$ and a total mass (including the dark matter) of $10^{15}\ h_{50}^{-1}\ M_\odot$ within a radius of $1\ h_{50}^{-1}$ Mpc. The total mass is consistent with the mass estimated from gravitational lensing observations. The ratio of hot gas mass to the total mass is thus only ∼4%(±2%, conservatively), lower than the ratio of the gas to total mass in Coma or other clusters within the same physical scale. These observations are consistent with a picture of cluster evolution in which an early starburst phase provides most of the intracluster iron and intracluster gas, and a substantial fraction of the baryonic matter is initially associated with galaxies.

Subject headings: dark matter — galaxies: clusters: individual (MS 0451.6−0305, MS 0016+16) — intergalactic medium — X-rays: galaxies

1. INTRODUCTION

X-ray spectra enable the determination of the temperature and metallicity of the hot gaseous atmospheres, or the intracluster media (ICM), of distant clusters of galaxies. The temperature of the gas reflects the depth of the potential well confining it and, therefore, the gravitational mass of the cluster. The metals in the gas trace the pollution of a primordial intracluster environment by galactic winds or stripping. Combined with imaging data from which gas densities and gas masses can be inferred, X-ray spectroscopy enables us to determine the gas mass fraction, which is a lower limit to the baryon fraction, and the mass of metals in the hot gas.

The galaxies respond to the same gravitational potential as the gas, and the gas particles and the galaxies should have approximately the same velocity dispersion. This hypothesis is supported by the correlation between ICM temperature and velocity dispersion of the member galaxies (e.g., Lubin & Bahcall 1993). Hydrodynamic cluster models suggest that the ICM temperature gives a reasonable estimate of the cluster mass (see Evrard 1990; Tsai, Katz, & Bertschinger 1994). The relationship between gas temperature and cluster mass can be tested by independent mass estimates obtained from analyses of gravitational lensing. In recent studies of weak shearing of the images of background galaxies (a method explained in Kaiser & Squires 1993), the lensing signature implies cluster gravitational masses in excess of the virial mass of clusters (Fahlman et al. 1994; Carlberg, Yee, & Ellingson 1994b; Bonnet, Mellier, & Fort 1994; Smail et al. 1995). In at least one cluster, MS 1224+2007, the mass derived from virial analysis of the cluster galaxies (Carlberg et al. 1994b) and the weak lensing signature are discrepant by a factor of 3 (Fahlman et al. 1994). When the X-ray temperature is consistent with the virial analysis, this discrepancy is difficult to understand. Systematic uncertainties such as neglecting nongravitational sources of gas heating, or subcluster mergers in the galaxy velocity distribution, would tend to overestimate, not underestimate, the gravitational mass. Strong magnetic fields (10–100 μG), as revealed by large rotation measures (Ge & Owen 1993; Perley & Taylor 1992; Dreher, Carilli, & Perley 1987; Taylor & Perley 1993) in some clusters, may supply some pressure support in the cluster core (Loeb & Mao 1994; Miralda-Escude & Babul 1995), but it is difficult to understand why the temperature and the velocity dispersion are correlated and numerically consistent if magnetic fields provide significant large-scale pressure support. In the cluster MS 0451.6−0305, we have the opportunity to compare the X-ray temperature (this work), the galaxy velocity dispersion (Carlberg et al. 1996), and the gravitational lensing mass (Luppino & Gioia 1995).

The iron abundance of the gas is a tracer of previous activity in the member galaxies: iron produced in star formation episodes is somehow removed from galaxies and mixed into the ICM (Arnaud et al. 1992b; David, Forman, & Jones 1991). By measuring the iron abundance of distant clusters, we can estimate when the dispersal of iron occurred—if distant clusters have systematically lower metallicities than nearby clusters, then the gas has been removed from the galaxies recently.

A long-term goal for observing distant X-ray clusters is to construct a temperature function, or better yet, a mass function of clusters of galaxies at redshifts of 0.5–1.0. Such a mass function will test models of large-scale structure. Since measuring a cluster temperature is more costly in terms of spacecraft time than measuring a cluster luminosity, cluster temperature functions would be easier to measure if the cluster luminosity predicted cluster temperature. At low redshift, the cluster luminosity is correlated with the cluster temperature (Mushotzky 1984; David et al. 1993). If the

same relation were true at high redshift, a first estimate of a high-redshift cluster mass function could be made from the cluster luminosities. Furthermore, cluster formation models predict a relationship between L_x and T_x that can change with redshift. A determination of the L_x-T_x relation at high redshift tests such models.

In this paper we present X-ray spectra of one of the most distant X-ray luminous clusters presently known, taken by the *Advanced Satellite for Cosmology and Astrophysics* (*ASCA*) (Tanaka, Inoue, & Holt 1994). This cluster, MS 0451−03, is the most luminous ($L_x = 2 \times 10^{45}\ h_{50}^{-2}$ ergs s^{-1}) cluster in the Extended Medium-Sensitivity Survey (EMSS; Gioia et al. 1990a; Stocke et al. 1991). A beautiful optical image of this cluster can be found in Luppino & Gioia (1995). The EMSS is a sample of 104 clusters from which evidence of negative evolution in the cluster luminosity function was derived, in the sense that there are fewer high-L_x clusters at redshifts 0.3–0.6 than at $z \sim 0.14$ (Henry et al. 1992; Gioia et al. 1990a; Castander et al. 1995). This negative evolution has been qualitatively confirmed by *ROSAT* X-ray observations of distant, optically selected clusters (Bower et al. 1994; Castander et al. 1994), which suggest that distant clusters of galaxies are underluminous in X-rays, given their optical richness.

We also observed MS 0451.6−0305 with the *ROSAT* Position Sensitive Proportional Counter (PSPC) (Donahue & Stocke 1995); we simultaneously analyze the PSPC spectral data and *ASCA* spectral data in this work. MS 0451.6−0305 was a target in the Canadian Network for Observational Cosmology (CNOC) consortium redshift survey of galaxy clusters (see Carlberg, Yee, & Ellingson 1994a).This cluster has a mean redshift of 0.539 and a velocity dispersion of 1371 km s^{-1}; both quantities were inferred from a sample of 51 cluster members (Carlberg et al. 1996). The 1 σ range for the dispersion as determined with the jackknife method is 1250–1449 km s^{-1} (Carlberg et al. 1996).

We assume that $H_0 = 50\ h_{50}$ Mpc $km^{-1}\ s^{-1}$ throughout this paper.

2. OBSERVATIONS AND DATA REDUCTION

ASCA executed a single, long (∼60,000 s) exposure of the cluster MS 0451.6−0305 during 1994 March 7–9. *ASCA* has four X-ray telescopes with which four independent data sets can be obtained. We extracted events from the two gas imaging spectrometers (GISs), gas-scintillation imaging proportional counters with energy resolution of 8% at 5.9 keV and 50′ diameter fields of view, and from the two solid-state imaging spectrometers (SISs), X-ray sensitive CCDs with energy resolutions of 2% at 5.9 keV and 22′ by 22′ fields of view. The SIS was read out in 4-CCD mode for these observations. The data analysis was restricted to one CCD.

We extracted clean X-ray-event lists by using a magnetic cutoff rigidity threshold of 6 GeV c^{-1} and the recommended minimum elevation angles (the angle between the target and the Earth's limb) and the bright Earth angle (the angle between the target and the day/night terminator on the Earth) to reject background contamination. The SIS0 and SIS1 data were screened further by using only SIS chip data grades of 0, 2, 3, and 4, which reject about 98% of cosmic-ray events, and by rejecting hot and flickering pixels. Light curves for each instrument were visually inspected, and time intervals with high background or data dropouts were excluded manually. The GIS3 was read out in an unusual manner during 1994 March, so the data had to be corrected by an *ASCA* Guest Observer Facility (GOF) data program "gis3bitfix." Because of the readout, the GIS3 spectral data has only 128 energy bins. The lower energy resolution does not affect our science. Both GIS spectra were then grouped into energy bins such that no energy bin had fewer than 16 counts. The SIS data were rebinned in the standard way to 512 spectral channels with Bright2Linear (see Day et al. 1995), with the lowest 13 channels flagged as bad. For data analysis, we then regrouped the SIS data by a factor of 2, restricting our analysis to those bins with statistically significant signal after background subtraction. Specifically, this procedure restricted the analysis of the SIS data to bins with greater than 10 net counts after background subtraction, and thus energies less than about 5–5.5 keV, and excluded the first 17 raw data channels from the analysis. The energy range is similar to that obtained by grouping the channels such that the minimum count rate per channel prior to background subtraction is 16. Events were selected from circular apertures 3′.5 (SIS) and 6′.0 (GIS), maximizing the signal over the background noise. Count rates for the GIS were about 0.040 counts s^{-1}, and for the SIS about 0.055 counts s^{-1}. We obtained useful exposure times of 26,800 and 35,860 s for the SIS0 and SIS1 detectors, respectively, and 52,200 s for each GIS detector.

Background estimates were taken from the detector regions surrounding the cluster detection and from summed deep background images supplied by the *ASCA* GOF. The deep background spectra were extracted with the same spatial and background removal filters used to extract the source data. The use of either the local background or the deep background did not affect the result in a statistically significant way.

We used XSPEC (v8.5), a spectral data analysis program within the software package XANADU available from the *ASCA* GOF. We fitted the spectral data from the four *ASCA* data sets and the PSPC data set, and their respective response files, which consist of a position-insensitive energy "redistribution" matrix and a position-sensitive effective area curve (see Day et al. 1995). The *ROSAT* PSPC data were grouped into bins as defined in Donahue & Stocke (1995). We used bins 5–30 in the fitting. The nominal fitted model was a Raymond-Smith thermal plasma absorbed by cold Galactic gas. The gas temperature, metallicity, soft absorption column from Galactic gas, and the normalization were allowed to vary. A reasonable fit was obtained with a reduced χ^2 of 1.1. A Mewe-Kaastra thermal plasma model was also fitted to the data with no significant change in the best-fit parameters. This consistency is expected, since the main differences between the two plasma codes occur for plasmas with L-shell Fe lines, that is, gas cooler than 2 keV. Cluster spectra from all four *ASCA* instruments were consistently fitted separately and well fitted simultaneously with the *ROSAT* data.

The best-fit X-ray temperature is $10.4^{+1.6}_{-1.3}$ keV, with an absorption column density of $3.0^{+0.7}_{-0.5} \times 10^{20}$ cm^{-2}, consistent with the Galactic value (Donahue & Stocke 1995). (All fit parameters are quoted with 90% confidence error estimates.) Fixing the Galactic column density at 3.2×10^{20} cm^{-2}, the best-fit $T_x = 10.4 \pm 1.2$ keV. The best-fit iron abundance, which relies mainly on the detection of the Fe K blend at rest energy ∼6.7 keV, is $0.15^{+0.11}_{-0.12}$ solar abundances. In Figure 1, we draw χ^2 contours at 68.3%,

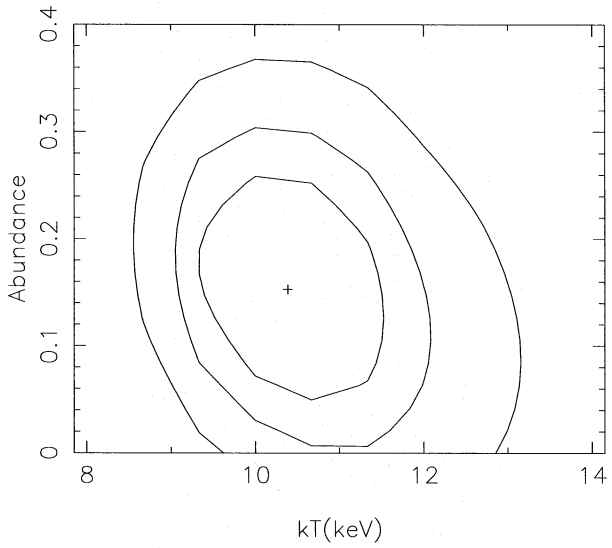

FIG. 1.—Contour plot of the two-dimensional χ^2 space for the fit of a Raymond-Smith thermal model to all five data sets discussed. The two parameters are X-ray temperature and iron abundance, as a fraction of the solar iron abundance, at 68.3%, 90%, and 99% confidence levels. The best-fit parameters are marked with a cross.

90% and 99% confidence levels for the cluster metallicity as a fraction of solar abundances and temperature in keV.

The initial analysis of the *ROSAT* PSPC data was presented in Donahue & Stocke (1995). Donahue & Stocke (1995) fitted a King profile $I \propto I_0[1 + (r/a)^2]^{-3\beta+0.5}$ to the PSPC surface brightness data for MS 0451.6−0305 out to a radius of 1 h_{50}^{-1} Mpc. If the gas is in hydrostatic equilibrium and isothermal, β (also known as $\beta_{\rm image}$ or $\beta_{\rm fit}$) is the ratio between the kinetic energy per galaxy particle and the thermal energy in the gas. They obtained $\beta = 1.06 \pm 0.16$ and core radius $a = 390^{+100}_{-70}\ h_{50}^{-1}$ kpc. (90% confidence limits are quoted.) The values of β and a are somewhat higher than in nearby clusters.

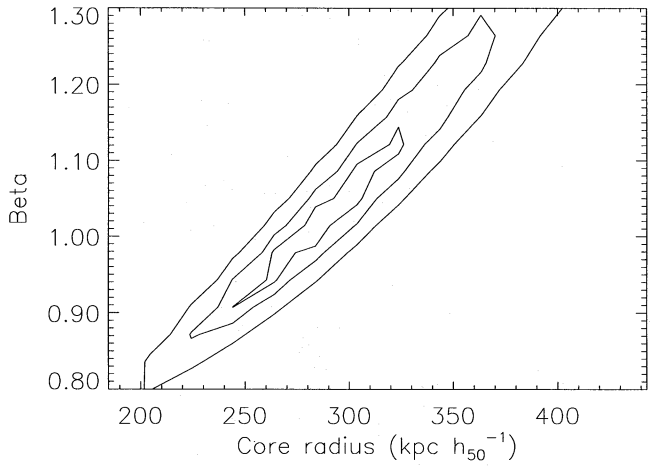

FIG. 2.—Contour plot of χ^2 for two parameters in the fit of a King model presented in this paper to the *ROSAT* PSPC surface brightness profile for the cluster MS 0451.6−0305. The two parameters are the slope β (see text) and the core radius a in kiloparsecs. (The third parameter is the central surface brightness.) The contours encompass the confidence levels of 68.3%, 90%, and 99%, respectively. The surface brightness profile is adequately fitted with a King profile convolved with the *ROSAT* PSPC PSF. The best-fit parameters are $a = 284$ kpc and $\beta = 1.01$, with a reduced χ^2 of 1.28.

We have subsequently performed a more sophisticated analysis of the PSPC data in order to see how the derived β and a parameters are affected by the instrumental point response. We convolved the King model with the on-axis PSPC point-spread function (PSF) as described in Hasinger et al. (1992), including the X-ray mirror scattering profile, the intrinsic spatial resolution of the PSPC, and focus and detector penetration effects. We derived somewhat different surface brightness parameters, but we will show that the gas masses, total cluster mass, and gas fraction are not very sensitive to these differences and therefore not very sensitive to uncertainties in the PSPC PSF. The best-fit parameters (with the PSF convolution) are $\beta = 1.01^{+0.27}_{-0.18}$ and $a = 280^{+85}_{-70}\ h_{50}^{-1}$ kpc, with a (deconvolved) central surface brightness of $(9.8^{+1.4}_{-0.6}) \times 10^{-6}$ ergs s^{-1} cm^{-2} sr^{-1}. These fit parameters are correlated such that a higher β requires a higher core radius a, and a lower β requires a lower core radius a, as shown on Figure 2, a plot of χ^2 contours for β and a.

3. DISCUSSION

3.1. *X-Ray Luminosity-Temperature Relation at High Redshift*

This very luminous cluster is one of the hottest clusters known. However, with a cluster rest-frame luminosity (2–10 keV) $L_x = 2.2 \times 10^{45}\ h_{50}^{-2}$ ergs s^{-1} within a 3.5 radius aperture, MS 0451.6−0305 is not any hotter than expected, given the L_x-T_x relation empirically derived for low-redshift clusters. The L_x-T_x relation fitted by Edge & Stewart (1991) predicts a 2–10 keV of luminosity of 2.2×10^{45} ergs s^{-1} for a temperature of 10.4 keV. In Figure 3, we plot temperature as a function of redshift for a sample of clusters with X-ray luminosities of $10^{44.9}$ ergs s^{-1} and greater (Arnaud et al. 1991). We also plot with triangles the temperatures of *any*

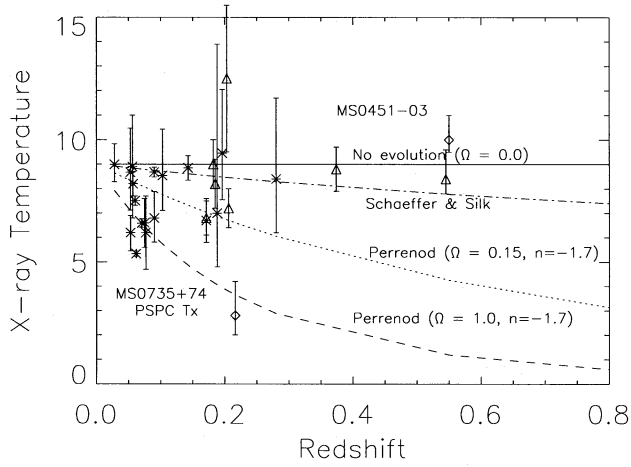

FIG. 3.—The temperatures and redshifts of X-ray luminous ($L_x > 10^{44.9}\ h_{50}^{-2}$ ergs s^{-1}) clusters from *Ginga* and *EXOSAT* observations (Arnaud et al. 1991) have been plotted with asterisks. Additionally, the triangles represent the temperatures and redshifts of all distant clusters observed in the PV phase of the *ASCA* mission (Yamashita 1994; Furuzawa et al. 1994; Bautz et al. 1994a). The temperature of MS 0451.6−0305, plotted here as a diamond, is consistent with no temperature evolution in the L_x-T_x relation since $z = 0.5$, at least for the most luminous clusters. The modified (see text) Perrenod (1980) and Schaeffer & Silk (1988) analytic models overlaid are predictions of the broad maximum of the cluster temperature distribution for a given redshift. They are plotted here to show the expectation that cluster temperatures rise with time for constant luminosity, given straightforward, self-similar gravitational collapse.

(regardless of luminosity) distant clusters with X-ray temperatures determined with *ASCA* (Bautz et al. 1994a; Yamashita 1994; Furuzawa et al. 1994). The triangular point in Figure 3 at $z = 0.55$ is MS 0016+16, whose *ASCA* temperature is 8.4 keV (Yamashita 1994; Furuzawa et al. 1994). The models plotted in Figure 3 reflect the expected maximum temperatures of the cluster temperature distribution as a function of redshift, normalized to a mean temperature for high-luminosity clusters at redshift zero. We modified the parameters in the analytic Perrenod (1980) models to reflect the cosmological parameters that best reproduce the evolution seen in the EMSS luminosity function (Henry et al. 1992; Evrard & Henry 1991). These models do not predict the temperature of a single cluster at a given redshift but rather represent the maximum of the temperature distribution at a given redshift. The nature of these Press-Schechter (1974) type of calculations means that this maximum has a broad dispersion, but they predict a general trend of cooler temperatures at higher redshift.

Self-similar models of gravitational collapse with no other heat source predict that $L_x \propto T_x^2(1+z)^{3/2}$ (Kaiser 1986). This "positive" evolution of the luminosity function with redshift means that clusters are expected to be more luminous, on average, at higher redshifts, contrary to the "negative" evolution observed in the EMSS sample. (The evolutionary trend of fewer X-ray luminous clusters at higher redshifts is confirmed by preliminary results from the RIXOS-*ROSAT* International X-ray and Optical Survey–cluster sample [Castander et al. 1995].) Self-similar models predict a correlation between L_x and T_x that is much shallower than observed, at least for low-redshift clusters (Edge & Stewart 1991). "Preheating" the gas (with galactic winds, for example) and requiring the central entropy to remain constant revises this relation to $L_x \propto T_x^{2.75}$, independent of redshift (Evrard & Henry 1991). Preheated models provide a better fit to the local L_x-T_x relationship, imply that the L_x-T_x relationship is constant with redshift, and may help explain the apparent lag between X-ray and optical evolution of clusters (see Donahue 1993 for a review of the issue or, more briefly, Henry 1995 and Postman et al. 1996 for an update on the lack of evolution seen in optically selected, distant cluster samples). Based on their Press-Schechter analysis for an open universe and their attempt to reproduce the redshift distribution of EMSS clusters, Oukbir & Blanchard (1996) suggest that high-redshift cluster temperatures may help distinguish between an open universe and a critical universe. They suggest that, for a critical universe, the L_x-T_x relation is either constant with redshift (a model that somewhat underpredicts the number of EMSS clusters at high redshift) or, if the L_x-T_x relation is allowed to vary, $L_x \propto (1+z)^{\alpha} T_x^3$, where $\alpha \sim +1$ for an $\Omega = 1$ model and $\alpha \sim -2.3$ for an $\Omega = 0.2$ model. While there is no physical argument as to why α may be 1 or -2.3, the questions concerning the evolution of the L_x-T_x relationship and the mean density of the universe may be settled empirically with the temperature measurement of a sample of high-redshift clusters.

Our observation of a single cluster at $z = 0.54$, coupled with the temperature measurements of 0016+16, suggest that the L_x-T_x relation does not evolve strongly with redshift, although, of course, this suggestion requires the confirmation of other cluster temperatures. A constant L_x-T_x relation is consistent with preheated/constant core entropy models.

3.2. *Hot Clusters and Models of Large-Scale Structure*

In the pioneering analytic work of Gunn & Gott (1972), they state that the present is the epoch of cluster formation. Twenty years later, Richstone, Loeb, & Turner (1992) pointed out that this is only true for high-density universes. In low-density universes, most clusters collapse and virialize at early times. In fact, by a redshift of 0.5, only 5% of present-day, $10^{15}\ M_\odot$ clusters in an $\Omega_0 = 1$ universe have formed, while in an $\Omega_0 = 0.05$ universe, nearly all $10^{15}\ M_\odot$ clusters have formed by that redshift (Richstone et al. 1992). Therefore, if $\Omega_0 = 1.0$, massive clusters should be rarer at epochs earlier than $z \sim 0.5$ than in the present.

Indeed, the mere existence of even a single hot cluster in the volume of the EMSS rules out a biased standard cold dark matter (CDM) model. The volume of space in the EMSS in which this cluster could have been detected is 8×10^8 Mpc^3. In the CDM model described by Arnaud et al. (1992a), the probability that a 10 keV cluster exists in such a volume is less than 10^{-3} if the biasing parameter $b > 1.5$. The reader is referred to excellent relevant discussions of CDM models and massive and distant X-ray clusters by Luppino & Gioia (1995) and Peebles, Daly, & Juszkiewicz (1989). Both of these papers agree that the existence of even a single massive ($10^{15}\ M_\odot$) cluster at redshifts of 0.5–0.6 is a problem for biased standard CDM. These papers based their conclusions on the discovery of distant X-ray luminous clusters (Luppino & Gioia 1995) or high-velocity–dispersion clusters (Peebles et al. 1989). With this cluster, we confirm the existence of a massive, distant cluster without assuming a relationship between L_x and T_x, or a lack of projection effects that may mimic high-velocity dispersions.

Since biased standard CDM models are not mutually consistent with the background fluctuations measured by *COBE* and smaller scale observations of galaxy motions, models that mix hot and cold dark matter, or flat, low-density models with a nonzero cosmological constant, have come into vogue. For example, Jing & Fang (1994) predicted cluster temperature functions for different epochs and for several large-scale structure models, including a mixed hot and cold dark matter model and a model with an inflationary constant, low-density cold dark matter. The difference between these two models is that the mixed model shows significant evolution (factor of 10) in the cluster temperature function, since $z = 0.5$, and a factor of 100 evolution, since $z \sim 0.8$. We cannot directly test current hydrodynamic simulations because MS 0451.6−0305 is so hot and luminous that temperature and luminosity functions derived from hydrodynamic simulations (Cen & Ostriker 1994; Jing & Fang 1994) for $z = 0.5$ do not contain it. In hierarchical models, such a hot cluster arises from an extremely high peak in the initial density fluctuation spectrum, which is very rare. The volume of a simulation needs to be very large to include such high peaks naturally. The comoving number density of such massive clusters should not be predicted from extrapolation of a theoretical temperature function to high temperatures.

3.3. *Gas Mass and Binding Mass within $R = 1\ h_{50}^{-1}$ Mpc*

The quantity $\beta_{\rm spec}$ is the dimensionless ratio between the velocity dispersion and the gas temperature. For MS 0451.6−0305, $\beta_{\rm spec}$ is 1.10 ± 0.16, consistent with the values found for low-redshift clusters. It is also consistent with the β derived from fitting a King profile to the X-ray surface

brightness profile (this work; see also Donahue & Stocke 1995). Consistency between β and β_{spec} is expected if a King profile describes the underlying galaxy distribution as well as that of the gas (see Bahcall & Lubin 1994); however, β and β_{spec} are nearly always different in low-redshift clusters.

For comparison, the famous cluster MS 0015.9+1609 (or CL 0016+16) at a redshift of 0.54 has a $\beta_{spec} = 1.19 \pm 0.15$, as inferred from the *ASCA* $T_x = 8.4^{+1.2}_{-0.6}$ keV (Yamashita 1994; Furuzawa et al. 1994) and the CNOC velocity dispersion of 1234 ± 128 km s^{-1} from 47 galaxies (Carlberg et al. 1996).[1] From *Einstein* IPC images, $\beta \sim 0.5$ for MS 0016+16 (White, Silk, & Henry 1981). *ASCA* surface brightness fits are somewhat steeper ($\beta = 0.8$; Yamashita 1994; Furuzawa et al. 1994), although this result is tentative pending investigations of the *ASCA* PSF. Evidence from the galaxy distribution (Dressler & Gunn 1992) and the ellipticity of the X-ray isophotes (Hughes & Birkinshaw 1994) indicates that MS 0016+16 may be undergoing a merger, or might even contain a cooling flow or X-ray point source (Hughes & Birkinshaw 1994) that would complicate the determinations of β_{spec} and β for this particular cluster.

Combining derived quantities from *ROSAT* and *ASCA* observations of MS 0451.6−0305 allows us to derive the total mass and the gas mass of this cluster within a radius $R = 1\ h_{50}^{-1}$ Mpc. The central gas density of MS 0451.6−0305 is $(4.8^{+0.8}_{-0.4}) \times 10^{-3}$ cm^{-3} ($\pm 10\%$), based on the deconvolved central surface brightness and, weakly, on the gas temperature. With the *ASCA* temperature, the integrated gas mass is then $(4.13^{+0.12}_{-0.08}) \times 10^{13}\ h_{50}^{-5/2}\ M_\odot$ for a gas density $\rho = \rho_0[1 + (r/a)^2]^{-3\beta/2}$. For a King function, the fitted β is correlated with the core radius a (see Fig. 2), such that the calculated gas mass is relatively insensitive to the triplet (β, a, central gas density) of parameters used. Formally, the uncertainties on the gas mass are very small, since the estimation of the gas mass is most sensitive to the integral of the flux within a 1 Mpc aperture. Measurement of this quantity is limited by photon statistics and only weakly dependent on the gas temperature. However, the framework for computing the gas mass assumes that the intracluster gas is smooth and unclumped. A clumpy gas has higher emission measure for a given mass, and therefore the gas mass may be somewhat lower than what we quote here. Donahue & Stocke (1995) note that any lumpiness in the emission at the resolution of the PSPC is limited to less than 10% of the total cluster emission; preliminary inspection of the HRI image of MS 0451.6−0305 suggests that the final analysis will constrain the lumpiness on much smaller scales, as well as rule out the existence of a significant active galactic nucleus or other point source in the core (Donahue et al. 1996). In the light of possible systematic uncertainties in the underlying clumpiness, the formal uncertainties of 1%–2% on the gas mass, as quoted above, are underestimates. Clumpiness as defined by $f_c = \langle n^2 \rangle / \langle n \rangle^2$ modifies the estimate of the gas mass such that $M_{gas} \propto f_c^{-1/2}$. Therefore, even if f_c is as high as 1.2, the gas mass estimated here is too high by only 10%. So we estimate that the uncertainty on the gas mass could be as high as 10%, almost entirely arising from the uncertainty on the clumpiness of the gas.

If the gas is nearly isothermal and in hydrostatic equilibrium with the cluster potential, the total mass within $R = 1$ Mpc is $1.0 \times 10^{14} \beta T(\mathrm{keV})[x^2/(1 + x^2)]\ M_\odot$, where $x = R/a$. This expression may not apply outside cluster radii of 1–3 h_{50}^{-1} Mpc, where the gas may not be in hydrostatic equilibrium. Recent cluster and group X-ray studies (e.g., David et al. 1994; Durret et al. 1994) and theoretical models (e.g., Tsai et al. 1994; Kang et al. 1994) suggest that the gas is nearly isothermal outside the influence of the cooling flow and inside several core radii. The cluster spectrum of MS 0451.6−0305 is adequately fitted by a single temperature model, and the surface brightness contours are rather regular. Therefore, isothermality is a reasonable assumption for this cluster within a radius of 1 Mpc. For MS 0451.6−0305, $M(R < 1\ \mathrm{Mpc}) = (9.7^{+3.8}_{-2.2}) \times 10^{14}\ h_{50}^{-1}\ M_\odot$. Encouragingly, this gravitational mass is consistent with the masses implied by *both* the virial estimate from the galaxy dispersion and the gravitational lens masses estimated by Luppino & Gioia (1995). This agreement suggests that the X-ray determination of the cluster mass interior to 1 Mpc is robust.

3.4. *Gas Fraction and Baryonic Fraction*

Donahue & Stocke (1995), using lower limits on T from *ROSAT* PSPC data, reported that MS 0451.6−0305 has an unusually low gas–to–total mass ratio of less than 17%. With the cluster temperature determined by *ASCA*, we confirm that MS 0451.6−0305 indeed has a low gas–to–total mass ratio: $M_{gas}/M_{total} = 4.1\% \pm 2\%\ h_{50}^{-3/2}$ within the central 1 Mpc h_{50}^{-1}. This uncertainty reflects the uncertainty in the temperature, the shape of the radial surface brightness profile, and the gas clumpiness. To be conservative, we estimate that the fractional uncertainty (90% confidence) may be as high as 30% for the total mass and 10% for the gas mass, resulting in a fractional uncertainty of 20% for the gas fraction. Since the gas fraction is small, the magnitude of the error bar on the percentage of the total mass is also small.

The gas fraction of $4.1\% \pm 2\%$ is significantly less than that within 1 Mpc of the center of Coma (16%)[2] and also less than that found inside $R = 1$ Mpc for 19 clusters observed by the *Einstein* satellite, 11%–23% (White & Fabian, 1995).

The high gas fractions found in clusters of galaxies are problematic for nucleosynthesis models (e.g., Walker et al. 1991) with $\Omega_0 = 1$, if the baryonic fraction in clusters of galaxies is not higher than in other places in the universe (White et al. 1993). Hydrodynamic models of cluster formation suggest that, if anything, the baryon fraction in clusters is less than the rest of the universe (e.g., Cen & Ostriker 1994.) The challenge of high gas fractions in clusters of galaxies is not resolved by the discovery of one cluster with a rather low hot gas fraction. The low gas fraction in MS 0451.6−0305 may imply: (1) that the assumption that the baryonic (gas and galaxies) fraction is relatively constant from cluster to cluster is incorrect, (2) that the radial dependence of the gas fraction on cluster radius makes this cluster appear gas poor, or (3) that most of the baryons in this particular cluster are found in the galaxies rather than the

[1] A somewhat higher velocity dispersion is calculated from velocities in Dressler & Gunn (1992) of 1696^{+291}_{-207} from spectroscopic measurements of 30 galaxies. See note in Hughes, Birkinshaw, & Huchra (1995).

[2] Briel, Henry, & Boehringer (1992) find a gas-to-total mass ratio of 30% inside 5 h_{50}^{-1} Mpc. We estimate the gas fraction inside 1 Mpc for purposes of comparison, by using the same set of assumptions as for MS 0451.6−0305, i.e., that the core temperature is isothermal and the gas traces the gravitational potential, and image parameters as fitted by Briel et al. ($n_0 = 2.89 \times 10^{-3}$, $\beta = 0.75 \pm 0.03$, $kT = 8.5$, and $a = 420\ h_{50}^{-1}$ kpc) to be 16%.

ICM. Theoretical work suggests that the first possibility can be ruled out. Numerical simulations with hydrodynamics (White et al. 1993) suggest that the baryonic fraction cannot vary dramatically from cluster to cluster.

In order to explore the second suggestion, we compare the gas fraction of this cluster with the gas fraction in nearby clusters on the same scale, as defined by radius, encircled mass, or number of core radii. The gas fraction in nearby clusters is a function of the radius, increasing at larger radii. First, we have already compared the gas fraction in MS 0451.6−0305 with similarly computed gas fractions at the same radius (1 h_{50}^{-1} Mpc) in nearby clusters (White & Fabian 1995.) Second, nearby cluster gas fractions appear to converge to an asymptotic limit of 25%–30% at encircled gravitational masses of 10^{15} $M_{\odot}$ (David, Jones, & Forman 1995); the encircled mass of MS 0451.6−0305 at 1 Mpc is 10^{15} $M_{\odot}$. And finally, White & Fabian (1995) show that, outside the core region of the potential, the gas fraction profiles are nearly constant. The core size for MS 0451.6−0305 is ∼280 kpc. Therefore, this cluster appears to have a statistically significant gas deficit in the central 1 Mpc.

This empirical comparison does not preclude the possibility that the *gradient* of the gas fraction (as a function of radius, number of core radii, or encircled mass) in MS 0451.6−0305 is different from that of nearby clusters. A gas fraction gradient may be caused by nongravitational heating in the cores of clusters that "puffs up" the gas with respect to the gravitational potential. However, the extremely high gas temperature, and its agreement with the virial velocity, limit the influence of any nongravitational heating in this cluster. Compressional heating from the cluster gravity alone heats the gas to 1.2×10^8 K. The heat provided by any known galactic source is trivial in comparison.

A true measure of the baryonic–to–dark matter ratio includes the galaxies' baryonic mass, but for low-redshift clusters, at least, the galactic contribution is considerably smaller than the gas contribution (David et al. 1991; Edge & Stewart 1991). Since the gas fraction for MS 0451.6−0305 is low, a universally constant baryonic fraction implies that the baryonic mass associated with the galaxies is high, or possibly located in a dust or gas shell surrounding the cluster. This last possibility is limited by the nondetection of excess absorption in this cluster. The 90% upper bound on the intrinsic absorption of MS 0451.6−0305 (fixing the Galactic value to 3.2×10^{20} cm^{-2}) is 1.5×10^{20} cm^{-2}. This column density limits the amount of cooler gas surrounding the cluster to 2.1×10^{13} $M_{\odot}$ $R_{\rm Mpc}^2$, less than $\frac{1}{3}$ of the amount of gas in the hot phase. Therefore, a hypothetical cool gas or dust shell cannot contribute significantly to the baryonic mass of this cluster unless the shell is much larger than 1 h_{50}^{-1} Mpc.

However, the third suggestion that some of the baryons are associated with the galaxies is still viable. At least some of the gas in this cluster has cycled through stars, since iron is detected. In order to explain the morphological mix of galaxies in clusters, Whitmore, Gilmore, & Jones (1993) suggested that galaxies or protogalaxies may disrupt and blend in with the ICM. Starburst winds in a population of dwarf spheroidals may remove all of their interstellar gas, enriching the ICM while squelching all subsequent star formation in the spheroidals (Trentham 1994). These calculations are mainly exercises in adjusting the cluster galaxy luminosity function in ways allowed (or not tested) by current observations. Number counts (or, better, luminosity functions) and optical/IR spectra of these cluster galaxies could reveal whether galaxies are unusually numerous or gas rich, say, from their blue colors or emission-line spectra. These ideas are all consistent with theoretical models assembled by David et al. (1991) and Arnaud et al. (1992b) to explain the high gas–to–stellar mass ratios and iron abundances in clusters of galaxies. Both David et al. (1991) and Arnaud et al. (1992b) suggest that the gas was blown out of galaxies in an early star formation phase, and both groups suggest that a peculiar stellar initial mass function is required to explain the high gas–to–stars ratio (although they did not agree on the form of this function).

3.5. *Metallicity*

The metallicity of the cluster gas (17% ± 11% solar), implied by the iron abundance is consistent with the metallicities (20%–30% solar) of the ICM in nearby clusters. The abundance of iron in MS 0451.6−0305 is apparently a little less than the 50% ± 10% reported in A370 at redshift 0.37 (Bautz et al. 1994b). The detection of intracluster iron at a redshift of 0.5 is consistent with an enrichment scenario in which early bursts of star formation propel metals out of the galaxies and into the ICM and/or completely disrupt the galaxy. It is not what one would expect from ram-pressure stripping that progressively removes gas from the galaxies since redshift 0.5. In the latter scenario, the gas of a distant cluster would be significantly poorer in metals, since ram-pressure stripping is an ongoing process and presumably would get more efficient with time as the ICM grew denser. The early star formation and enrichment picture is supported by *ASCA* observations in which the element ratios (particularly oxygen/iron) in nearby clusters are typical of Type II supernovae enrichment, rather than Type I (Mushotzky 1994).

4. SUMMARY

We have reported on *ASCA* observations of a distant ($z = 0.54$) cluster of galaxies, MS 0451.6−0305. The gas in this cluster is very hot, 10.4 ± 1.2 keV, implying a cluster mass interior to 1 Mpc of ∼10^{15} $M_{\odot}$. This mass and temperature is consistent with the galaxy velocity dispersion and lensing mass, implying that the gas and the galaxies are in nearly virial equilibrium in the gravitational potential. The gas fraction interior to 1 Mpc is 4.1% ± 2%, at least a factor of 2 lower than in nearby clusters within identical length or mass scales. The emission-weighted metal abundance in the gas is somewhat lower than, but consistent with, metal abundances of gas in nearby clusters. This cluster is hotter and more massive than Coma or CL 0016+16. The mere existence of such a massive cluster in the volume surveyed by the EMSS places a strong constraint on cosmological parameters in cluster formation models such as biased CDM (Luppino & Gioia 1995; Arnaud et al. 1991). Our observation that the X-ray temperature is consistent with the cluster luminosity, according to the local L_x-T_x relationship, implies that the high-luminosity end of this relationship is constant out to at least redshifts of 0.5. This also rules out some cluster formation models, such as the self-similar models (Kaiser 1986), but is consistent with models in which the gas is preheated before falling into the deepening cluster potential (Evrard & Henry 1991; Kaiser 1991). Finally, the low gas fraction and the

modest iron abundance are consistent with models for the origin of the ICM in which much of the ICM is processed by stars and blown out by superwinds powered by star formation, with or without galaxy destruction.

M. D. was supported by a Carnegie Fellowship, NASA *ROSAT* grant NAG 5-2021, NASA *ASCA* grant NAG 5-2570, and an Institute Postdoctoral Fellowship supported by the Space Telescope Science Institute. She thanks the CNOC team and Ray Carlberg for releasing their velocity dispersion results in advance of publication. She also thanks John Stocke and G. Mark Voit for their reading of the manuscript. M. D. is grateful to the referee, who provided comments and suggestions that improved the quality of this paper.

REFERENCES

Arnaud, M., Hughes, J. P., Forman, W., Jones, C., Lachieze-Rey, M., Yamashita, K., & Hatsukade, I. 1992a, ApJ, 390, 345
Arnaud, M., Lachiéze-Rey, M., Rothenflug, R., Yamashita, K., & Hatsukade, I. 1991, A&A, 243, 56
Arnaud, M., Rothenflug, R., Boulade, O., Vigroux, L., & Vangionflam, E., 1992b, A&A, 254, 49
Bahcall, N. A., & Lubin, L. 1994, ApJ, 426, 513
Bautz, M. W., Crew, G. B., Gendreau, K. C., Mushotzky, R. F., Arnaud, K. A., Fabian, A. C., Yamashita, K., & Tawara, Y. 1994a, in New Horizon of X-Ray Astronomy, ed. F. Makino & T. Ohashi (Tokyo: Universal Academy Press), 285
Bautz, M. W., Mushotzky, R., Fabian, A. C., Yamashita, K., Gendreau, K. C., Arnaud, K. A., Crew, G. B., & Tawara, Y. 1994b, PASJ, 46, L131
Bonnet, H., Mellier, Y., & Fort, B. 1994, ApJ, 427, L83
Bower, R. G., Böhringer, H., Briel, U. G., Ellis, R. S., Castander, F. J., & Couch, W. J. 1994, MNRAS, 268, 345
Briel, U. G., Henry, J. P., & Boehringer, H. 1992, A&A, 259, L31
Carlberg, R. G., Yee, H. K. C., & Ellingson, E. E. A. 1994a, JRASC, 88, 39
———. 1994b, ApJ, 437, 63
Carlberg. R. G., Yee, H. K. C., Ellingson, E., Abraham, R., Gravel, P., Morris, S., & Pritchet, C. 1996, ApJ, 462, 32
Castander, F. J., Ellis, R. S., Frenk, C. S., Dressler, A., & Gunn, J. E. 1994, ApJ, 424, L79
Castander, F. J., et al. 1995, Nature, 377, 39
Cen, R., & Ostriker, J. P. 1994, ApJ, 429, 4
David, L. P., Forman, W., & Jones C. 1991, ApJ, 380, 39
David, L. P., Jones, C., & Forman, W. 1995, ApJ, 445, 578
David, L. P., Jones, C., Forman, W., & Daines, S. 1994, ApJ, 428, 544
David, L. P., Slyz, A., Jones, C., Forman, W., & Vrtlek, S. D. 1993, ApJ, 412, 479
Day, C., Arnaud, K., Ebisawa, K., Gotthelf, E., Ingham, J., Mukai, K., & White, N. 1995, The ABC Guide to *ASCA* Data Reduction, Fourth Version, available by request from the *ASCA* GOF (Greenbelt: NASA/GSFS)
Donahue, M. 1993, in Evolution of Galaxies and Their Environment, ed. J. M. Shull & H. A. Thronson, Jr. (Dordrecht: Kluwer), 409
Donahue, M., & Stocke, J. T. 1995, ApJ, 449, 554
Donahue, M., et al. 1996, in preparation
Dreher, J. W., Carilli, C. L., & Perley, R. A. 1987, ApJ, 316, 611
Dressler, A., & Gunn, J. E. 1992, ApJS, 78, 1
Durret, F., Gerbal, D., Lachieze-Rey, M., Lima-Neto, G., & Sadat, R. 1994, A&A, 287, 733
Edge, A. C., & Stewart, G. C. 1991, MNRAS, 252, 414
Evrard, A. E. 1990, ApJ, 363, 349
Evrard, A. E., & Henry, J. P. 1991, ApJ, 383, 95
Fahlman, G., Kaiser, N., Squires, G., & Woods, D. 1994, ApJ, 437, 56
Furuzawa, A., Yamashita, K., Tawara, Y., Tanaka, Y., & Sonobe, T. 1994, in New Horizon of X-Ray Astronomy, ed. F. Makino & T. Ohashi (Tokyo: Universal Academy Press), 541
Ge, J. P., & Owen, F. N. 1993, AJ, 105, 778
Gioia, I. M., Henry, J. P., Maccacaro, T., Morris, S. L., & Stocke, J. T. 1990a, ApJ, 356, L35
Gioia, I. M., Maccacaro, T., Schild, R. E., Wolter, A., & Stocke, J. T. 1990b, ApJS, 72, 567
Gunn, J. E., & Gott, J. R. 1972, ApJ, 176, 1
Hasinger, G., Turner, T. J., George, I. M., & Boese, G. 1992, OGIP Calibration Memo CAL/ROS/92-001
Henry, J. P. 1995 Nature, 377, 13
Henry, J. P., & Arnaud, K. A. 1991, ApJ, 372, 410
Henry, J. P., Gioia, I. M., Maccacaro, T., Morris, S. L., & Stocke, J. T. 1992, ApJ, 386, 408
Hughes, J. P., & Birkinshaw, M. 1994, in AIP Conf. Proc. 313, The Soft X-Ray Cosmos, ed. E. M. Schlegel & R. Petre (New York: AIP), 378
Hughes, J. P., Birkinshaw, M., & Huchra, J. P. 1995, ApJ, 448, L93
Jing, Y. P., & Fang, L. Z. 1994, ApJ, 432, 438
Kaiser, N. 1986, MNRAS, 222, 323
———. 1991, ApJ, 383, 104
Kaiser, N., & Squires, G. 1993, ApJ, 404, 441
Kang, H., Cen, R., Ostriker, J., & Ryu, D. 1994, ApJ, 428, 1
Loeb, A., & Mao, S. 1994, ApJ, 435, L109
Lubin, L. M., & Bahcall, N. A. 1993, ApJ, 415, L17
Luppino, G. A., & Gioia, I. M. 1995, ApJ, 445, L77
Miralda-Escude, J., & Babul, A. 1995, ApJ, 449, 18
Mushotzky, R. 1984, Phys. Scr., T7, 157
———. 1994, in New Horizon of X-Ray Astronomy, ed. F. Makino & T. Ohashi (Tokyo: Universal Academy Press), 243
Oukbir, J., & Blanchard, A. 1996, A&A, submitted
Peebles, J., Daly, R., & Juszkiewicz, R. 1989, ApJ, 347, 563
Perley, R. A., & Taylor, G. 1991, AJ, 101, 1623
Perrenod, S. C. 1980, ApJ, 236, 373
Postman, M., Lubin, L., Gunn, J. E., Oke, J. B., Hoessel, J. G., Schneider, D. P., & Christensen, J. A., 1997, AJ, 111, 615
Press, W., & Schechter, P. 1974, ApJ, 187, 425
Richstone, D., Loeb, A., & Turner, E. L. 1992, ApJ, 393, 477
Schaeffer, R., & Silk, J. 1988, ApJ, 333, 509
Smail, I., Ellis, R. S., Fitchett, M. J., & Edge, A. C. 1995, MNRAS, 273, 277
Stocke, J. T., Morris, S. L., Gioia, I. M., Maccacaro, T., Schild, R., Wolter, A., Fleming, T. A., & Henry, J. P. 1991, ApJS, 76, 813
Tanaka, Y., Inoue, H., & Holt, S. S. 1994, PASJ, 46, L37
Taylor, G. B., & Perley, R. A. 1993, ApJ, 416, 554
Trentham, N. 1994, Nature, 372, 157
Tsai, J. C., Katz, N., & Bertschinger, E. 1994, ApJ, 423, 553
Walker, T. P., Steigman, G., Schramm, D. N., Olive, K. A., & Kang, H. S. 1991, ApJ, 376, 51
White, D. A., & Fabian, A. C. 1995, MNRAS, 273, 72
White, S. D. M., Navarro, J. F., Evrard, A. E., & Frenk, C. S. 1993, Nature, 366, 429
White, S. D. M., Silk, J., & Henry, J. P. 1981, ApJ, 251, L65
Whitmore, B. C., Gilmore, D. M., & Jones, C. 1993, ApJ, 407, 489
Yamashita, K. 1994, in New Horizon of X-Ray Astronomy, ed. F. Makino & T. Ohashi (Tokyo: Universal Academy Press), 279